NEOPLASIA
www.neoplasia.com

Volume 14 Number 11 November 2012 pp. 1032–1042 1032

Role of Proprotein Convertases in Prostate Cancer Progression[1,2]

Frédéric Couture*, François D'Anjou*, Roxane Desjardins*, François Boudreau† and Robert Day*

*Institut de Pharmacologie de Sherbrooke, Department of Surgery/Urology, Université de Sherbrooke, Sherbrooke, Québec, Canada; †Department of Anatomy and Cell Biology, Université de Sherbrooke, Sherbrooke, Québec, Canada

Abstract

Better understanding of the distinct and redundant functions of the proprotein convertase (PC) enzyme family within pathophysiological states has a great importance for potential therapeutic strategies. In this study, we investigated the functional redundancy of PCs in prostate cancer in the commonly used androgen-sensitive LNCaP and the androgen-independent DU145 human cell lines. Using a lentiviral-based shRNA delivery system, we examined *in vitro* and *in vivo* cell proliferation characteristics of knockdown cell lines for the endogenous PCs furin, PACE4, and PC7 in both cell lines. Of the three PCs, only PACE4 was essential to maintain a high-proliferative status, as determined *in vitro* using XTT proliferation assays and *in vivo* using tumor xenografts in nude mice. Furin knockdowns in both cell lines had no effects on cell proliferation or tumor xenograft growth. Paradoxically, PC7 knockdowns reduced *in vitro* cellular proliferation but had no effect *in vivo*. Because PCs act within secretion pathways, we showed that conditioned media derived from PACE4 knockdown cells had very poor cell growth–stimulating effects *in vitro*. Immunohistochemistry of PACE4 knockdown tumors revealed reduced Ki67 and higher $p27^{KIP}$ levels (proliferation and cell cycle arrest markers, respectively). Interestingly, we determined that the epidermal growth factor receptor signaling pathway was activated in PC7 knockdown tumors only, providing some explanations of the paradoxical effects of PC7 silencing in prostate cancer cell lines. We conclude that PACE4 has a distinct role in maintaining proliferation and tumor progression in prostate cancer and this positions PACE4 as a relevant therapeutic target for this disease.

Neoplasia (2012) 14, 1032–1042

Introduction

The mammalian proprotein convertases (PCs) form a family of enzymes that is responsible for the activation of numerous protein precursors within the secretory pathway. Nine different PCs have been identified, namely, furin, PACE4, PC1/3, PC2, PC4, PC5/6, PC7, PCSK9, and SKI-1/S1P [1,2]. Only the first seven of these serine proteases process substrates with an optimal PC recognition sequence R-X-K/R-R↓, whereas the minimal consensus sequence is R-X-X-R↓. A variety of substrates have been described such as precursors of hormones, enzymes, growth factors, receptors, cell membrane proteins, and plasma proteins but also a number of pathogenic proteins such as viral glycoproteins and bacterial toxins. There is growing evidence for the involvement of PCs in various cancer types, including roles in each of the biologic capabilities acquired during the multistep development of human tumors [3]. These biologic capabilities include proliferative signaling [4], evading growth suppressors [5], enabling replicative immortality [6], inducing angiogenesis [7], and activating invasion and metastasis [8].

Abbreviations: PC, proprotein convertase; RPMI, Roswell Park Memorial Institute medium; FBS, fetal bovine serum; EGF(R), epidermal growth factor (receptor); PSA, prostate-specific antigen; MVD, microvessel density; NT, non-target

Address all correspondence to: Dr Robert Day, Institut de Pharmacologie de Sherbrooke, Faculté de Médecine et des Sciences de la Santé, Université de Sherbrooke, 3001, 12e Ave. Nord, Sherbrooke, Québec J1H 5N4, Canada. E-mail: robert.day@usherbrooke.ca

[1]This work was awarded by Prostate Cancer Canada and is proudly funded by Movember Foundation grant 2012-951. This work was also supported by the Ministère du Développement Économique, de l'Innovation et de l'Exportation du Québec and the Canadian Institutes of Health Research. F.C. holds a graduate student scholarship from the Fonds de Recherche du Québec-Santé (FRQS). F.B. is a senior scholar from the FRQS. R.D. and F.B. are members of the Centre de Recherche Clinique Étienne-LeBel (Sherbrooke, Québec, Canada).

[2]This article refers to supplementary materials, which are designated by Tables W1 and W2 and Figures W1 and W2 and are available online at www.neoplasia.com.

Received 21 August 2012; Revised 24 September 2012; Accepted 27 September 2012

DOI 10.1593/neo.121368

Prostate cancer is a worldwide health problem and is the second leading cause of cancer deaths behind lung cancer in North American men [9]. Prostate cancer threatens the life of patients by its ability to overcome initial hormone therapies as it becomes castration resistant, which then limits traditional therapeutic interventions and leads to metastasis and poor prognosis. Thus, the identification and validation of novel pharmacological targets suitable for the treatment of such aggressive tumors represents an unmet need.

In a recent study, we showed that PACE4 was highly overexpressed in prostate cancer tissues [10]. PACE4 silencing, based on an engineered delta-ribozyme approach, in the androgen-independent DU145 prostate cancer model cell line resulted in reduced proliferation and tumor xenograft progression in athymic nude mice. We thus hypothesized that PACE4 may be a potential druggable target for prostate cancer. If this is the case, then further information on the role of co-expressed PCs in prostate cancer becomes essential as redundancy among the PCs is well established. Thus, in prostate cancer, we raise the question as to whether the sole inhibition of PACE4 would suffice to produce beneficial effects or whether other PCs should also be considered for inhibition to attain this goal. Therefore, in the present study, we examined the role of other PCs in the cellular proliferation and tumor progression of prostate cancer cells using molecular silencing methods. We used lentivirus-delivered shRNAs to knockdown furin, PC7, and PACE4 in the androgen-sensitive LNCaP cell line and also in the androgen-independent DU145 cell line and then examined cell proliferation and tumor growth characteristics, *in vitro* and *in vivo*.

Materials and Methods

Cell Culture

All cell lines used were obtained from ATCC (Manassas, VA). Human prostate cancer cell lines DU145 and LNCaP were maintained in Roswell Park Memorial Institute medium (RPMI 1640) supplemented with either 5% fetal bovine serum (FBS; Wisent Bioproducts, St Bruno, Canada) for DU145 or 10% for LNCaP. Human embryonic kidney 293FT cells (HEK293FT; Invitrogen, Carlsbad, CA) were grown in Dulbecco's modified Eagle's medium and 10% FBS supplemented with 6 mM glutamine and 500 μg/ml G418. HT1080 cells were grown in Dulbecco's modified Eagle's medium with 10% FBS. Cells were grown at 37°C in a water-saturated atmosphere with 5% CO_2.

Lentivirus Production and shRNA Transduction

Production of lentiviral particles containing the MISSION RNAi pLKO.1-puro vector (see Table W1 for shRNA sequences) was carried out in HEK293FT cells following manufacturer's instructions (Sigma-Aldrich, St Louis, MO). Viral titers were calculated using a serial dilution approach with HT1080 cells. Lentivirus transductions were carried out in 6-well plates with 6×10^4 cells or in 12-well plates with 5×10^4 cells (for DU145 and LNCaP, respectively) with a multiplicity of infection of 3. After 2 days, the infected cells were selected using growth medium containing 1 or 2 μg/ml puromycin, respectively, for LNCaP and DU145 cells. Cells were further cultured under selective pressure using media with these puromycin concentrations for culture on passages. On characterization, the selected polyclonal cell populations were used for further studies to avoid any artifact associated with individual clone selection [11]. Cell populations were cultured for 10 to 12 passages before being discarded.

Real-time Quantitative Polymerase Chain Reaction

Total RNA was extracted using the Qiagen RNA Isolation Kit (Qiagen, Valentia, CA). RNA quality was assessed using an Agilent Bioanalyzer with RNA Nano Chips (Agilent Technologies, Palo Alto, CA). For tumor RNA isolation, Trizol-chloroform extractions (Invitrogen) were carried out on tissues crushed in liquid nitrogen. Real-time quantitative polymerase chain reaction (qPCR) reactions were performed as previously described [10]. Briefly, 1 μg of RNA was reverse transcribed and qPCR analysis reactions were done with a Stratagene Mx3005P instrument. All primers used are listed in Table W2. Relative expression levels were calculated using β-actin as a reference gene with the formula $(1 + \text{amplification efficiency})^{-\Delta(\Delta CT)}$. Experiments were done in duplicate in three independent experiments ($n = 3$).

XTT Proliferation Assay

The cellular proliferation was measured with the colorimetric XTT Cell Proliferation Kit II following the manufacturer's instructions (Roche Applied Science, Indianapolis, IN). Briefly, cells were seeded (1000 cells/well for DU145 and 3000 cells/well for LNCaP) in four 96-well plates in triplicate. For the next days, a plate was revealed after a 4-hour incubation with the reagent solution. Absorbance values were measured at a wavelength of 490 nm with a reference at 690 nm in a microplate reader (SpectraMax190; Molecular Devices, Sunnyvale, CA). For each time point, data were reported as percentage of mean values measured at 24 hours with corrections applied for the respective blanks (complete medium).

Conditioned Growth Medium Preparation and Proliferation Induction Measurements

As previously described, conditioned media were produced from four 10-cm plates seeded with 1.0×10^6 cells in complete growth media [10]. The next day, the cells were washed twice with phosphate-buffered saline (PBS) and the growth media were replaced with 5 ml of serum-free RPMI for 1 hour. The conditioned media were then collected, filtered through 0.45-μm filters, and concentrated to a final volume of 350 μl with Amicon Ultra centrifugal filter devices (Millipore, Billerica, MA) with a 3-kDa molecular weight cutoff. Fresh RPMI medium was treated the same way as a control.

The potential of these concentrated media to induce proliferation was measured as follows: for DU145, 50 μl of conditioned media was applied on control or shRNA-transfected cells seeded in 96-well plates (2000 cells/well) in triplicate. After a 48-hour incubation period, 12.5 μl of Thiazolyl Blue Tetrazolium Blue (MTT) compound (5 mg/ml; Sigma-Aldrich) was added to each well (25 μl for LNCaP). After a 4-hour incubation, the medium was carefully removed and cells were solubilized with a mixture of isopropanol/1N HCl (25:1). For LNCaP cells, 4500 cells/well were used and 50 μl of conditioned media was added to 50 μl of fresh 5% FBS medium.

The absorbance was measured at a wavelength of 550 nm with a reference at 650 nm in a microplate reader. MTT was used instead of XTT because the latter would have required a specific background subtraction for each conditioned medium generated.

Western Blot Analysis

Total proteins were extracted from excised tumors crushed in liquid nitrogen using RIPA buffer supplemented with protease inhibitors (complete Mini; Roche). Protein concentrations were determined using a BCA Protein Assay Kit (Pierce, Rockford, IL) and

50 μg of protein samples were separated on a sodium dodecyl sulfate–polyacrylamide gel electrophoresis and transferred to a nitrocellulose membrane (Hybond; GE Healthcare, Chalfont St Giles, United Kingdom). Before immunodetection, membranes were blocked with 5% (wt/vol) BSA in a 0.1% Tween-PBS solution. Membranes were then incubated with anti-actin (NeoMarkers, Fremont, CA), anti–epidermal growth factor receptor (EGFR; Signalway Antibody, SAB, Pearland, MD), anti–phospho-Ser^{1070}–EGFR (SAB) primary antibody overnight at 4°C followed by incubation with a goat anti-rabbit or anti-mouse IgGs coupled to IRDye800 (LI-COR Biosciences, Lincoln, NE). Immunodetection was then performed using an infrared imager (Odyssey Imager, LI-COR Biosciences). Relative protein expression levels were calculated using the ImageJ software.

Human Tumor Xenograft Models

Four- to six-week-old male athymic nude mice (Nu/Nu; Charles River Laboratories, Lasalle, Canada) were inoculated subcutaneously on the opposite sides of the flanks and shoulders with 2.0 and 3.0 × 10^6 cells per inoculum, respectively, for LNCaP and DU145 (five mice per group). Cells were grown in complete media and harvested at their exponential growing state. Mice were housed under pathogen-free conditions and the inoculations were done under isoflurane anesthesia conditions in a laminar flow hood. For LNCaP cells only, 100 μl of cell suspension in cold PBS was mixed with 100 μl of matrigel before injection (BD Biosciences, Bedford, MA). Xenografts were measured three times per week and volumes (V) were determined using the formula $V = (L \times W^2) \times \pi/6$, where L is the tumor length and W is the tumor width. For prostate-specific antigen (PSA) monitoring, blood samples were collected weekly in heparinized micro-hematocrit capillary tubes (Thermo Fisher Scientific, Waltham, MA) from mice saphenous vein. Blood samples were kept on ice with 10 U of heparin until a 10-minute centrifugation at 3500*g* was performed to collect plasma. Plasmatic and cell growth medium PSA concentrations were determined using a PSA ELISA Test Kit (ClinPro International, Union City, CA).

Immunohistochemistry

On mice sacrifice, tumors were eradicated, formalin fixed, and paraffin embedded. Immunohistochemistry (IHC) was performed on 5-μm sections in the Department of Pathology, Centre Hospitalier Universitaire de Sherbrooke (CHUS; Sherbrooke, Canada) using the standard streptavidin-biotin-peroxidase immunostaining procedure with a Ventana NexES autostainer and the solvent-resistant DAB Map Detection Kit (Ventana Medical System, Tucson, AZ). Antibodies (p27^{KIP}, 1:100 and EGFR, 1:800) and ready-to-use solutions (p53, PSA, Ki67, CD34) were purchased from Dako Canada (Burlington, Canada).

For Ki67 proliferation index determination, up to five representative fields containing an average of 150 cells were captured for each analyzed tumor and were used to manually count cells with positive nuclear staining that were reported on the total number of cells per field. For immunostaining quantifications, the yellow channel of a CMYK color model for each picture taken on a SuperCoolscan 9000 (Nikon, Tokyo, Japan) was extracted using Fiji software (Open Source) and used to quantify staining density relative to tumor area [12]. To avoid quantification of any off-tumor area (e.g., skin and fat), we counterstained tumor areas using hematoxylin and eosin (H&E) additionally to p53 or PSA as a positive marker for DU145 and LNCaP cells, respectively. Pictures with ×100 and ×400 magnification were acquired using an Axioskop 2 phase-contrast microscope (Carl Zeiss, Thornwood, NY) and processed using Image Pro software (Media Cybernetics, Bethesda, MD). Microvessel densities (MVDs) were calculated by counting the number of microvessels positive for CD34 immunostaining divided by their respective tumor area. The tumor areas were determined using the ImageJ software with ×15 magnified images.

Statistical Analysis

All experiments were repeated at least three times, and the results were expressed as mean ± SEM. Statistical analysis was done using Student's t test to calculate P values.

Results

Knockdown of Endogenous PCs in Prostate Cancer Model Cell Lines

In a previous study, we characterized PCs only in the DU145 cell line, showing PACE4, furin, and PC7 mRNA expression [10]. Herein, we first characterized PC expression in DU145 and LNCaP prostate cancer cell lines and demonstrated a similar PC expression pattern, with the exception that LNCaP expressed three-fold higher levels of PACE4 than the DU145 (Figure 1*A*). This characterization of PC expression levels in LNCaP and DU145 cells was carried out to define the PC targets for the subsequent molecular silencing studies. Therefore, we decided to develop knockdown LNCaP and DU145 cell lines for furin, PACE4, and PC7. Considering the number of cell lines required, we chose an RNA interference approach using lentiviral-based delivery system. Viral particles coding for shRNAs specific to each PC were prepared from five MISSION shRNA vectors available from Sigma-Aldrich. The best shRNA for each PC target (i.e., furin, PACE4, and PC7) was selected on the basis of their silencing efficiency (Figure W1 and Table W2).

Stable knockdown polyclonal cell lines were obtained through puromycin selection, whereas the non-target (NT) shRNA and the empty PLKO vectors were both used as controls (Figure 1, *B* and *C*). The resulting puromycin-resistant cell populations were assessed for their expression level of each endogenous PC by real-time qPCR on total RNA. When compared to the NT control cells, significant knockdowns were obtained for all cell lines, with less than 25% residual expression remaining and without major compensatory overexpression of any other PC. In the DU145 cells, knockdown levels for furin, PACE4, and PC7 were, respectively, 93%, 78%, and 87% of control cells expression levels. For the LNCaP cell lines, PC knockdown levels were, respectively, 92%, 85%, and 93% when compared to controls. As empty vector–infected cell lines were exempt of any significant variation in PC expression levels, the silencing method was considered valid and reliable. We validated the stability of the mRNA knockdowns for up to 30 passages (data not shown).

Effect of PC Knockdowns on Cell Proliferation

To determine the effects of endogenous PC knockdowns on the growth capabilities of LNCaP and DU145 cell lines, we measured their proliferation rates using the XTT assay on a 96-hour time course. This colorimetric assay allows the direct measurement of cellular proliferation rates by monitoring the metabolic reduction of the reagent in a soluble formazan. As shown in Figure 2*A*, DU145 cell lines silenced for PACE4 or PC7 showed significantly reduced proliferation

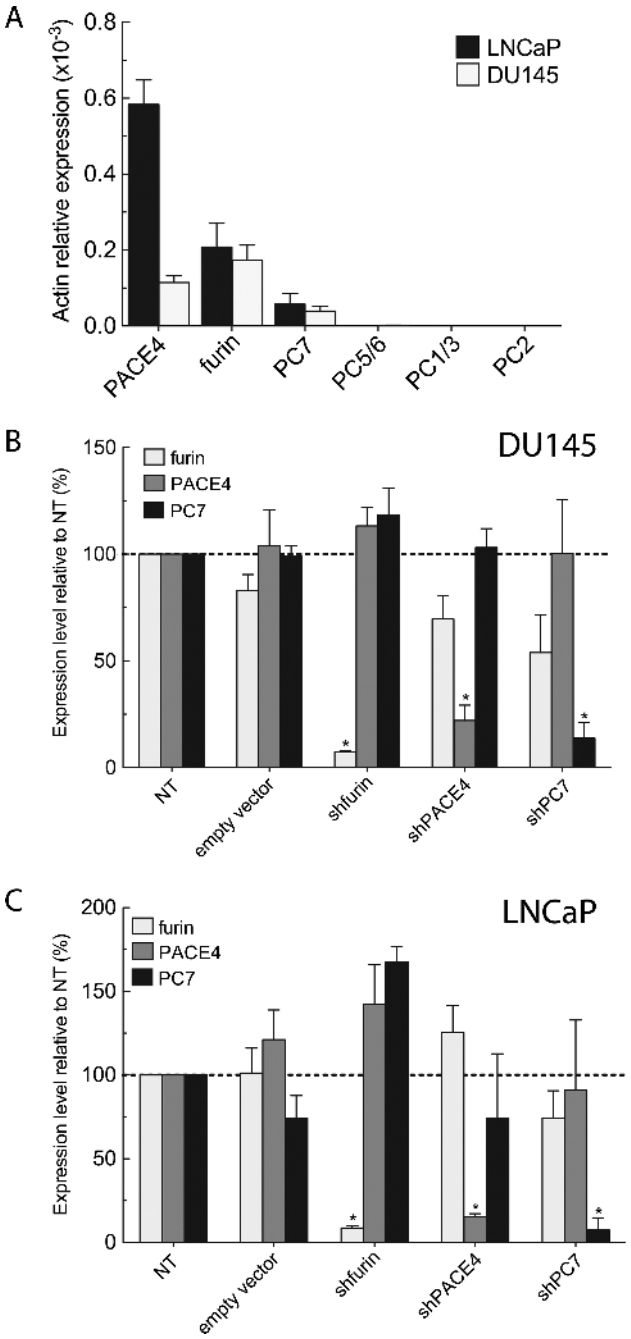

Figure 1. Stable knockdown of endogenous PCs in DU145 and LNCaP prostate cancer cells. (A) Real-time qPCR measuring relative endogenous PC mRNA expression levels in DU145 and LNCaP wild-type cells. PC knockdown assessment by real-time qPCR on DU145 (B) and LNCaP (C) shRNA–expressing cell lines. The mRNA expression levels of other endogenously co-expressed PCs (furin, PACE4, and PC7) were also determined. Data are means ± SEM ($n = 3$) of mRNA levels relative to NT using β-actin as reference gene. *$P < .05$.

rates after 72 and 96 hours with overall reductions of, respectively, 50% and 68% relative to NT control cells. No significant difference was observed for the DU145 furin knockdown cell line. Similar results were obtained with the LNCaP cell lines, as significant differences could be observed after 48 hours (Figure 2*B*). Reductions in proliferation rates were of about 45% and 30% for the LNCaP PACE4 and PC7 knockdowns, respectively, with no significant difference for the LNCaP furin knockdowns.

Secreted Growth Factors Are Implicated in PC-mediated Proliferation Effects

As PCs act in secretory pathways, we evaluated the growth induction potential of conditioned media derived from the knockdown cells of both DU145 and LNCaP. We hypothesized that any proliferation rate reductions in PC knockdown cells could be due to reduced self-sustaining growth factor activity. The reduction of growth factor activity would be the result of reduced processing by the PC knockdown. Serum-free conditioned media were produced under short incubation conditions to prevent cell quiescence and possible secretome degradation and to avoid the application of exogenous growth factors. After concentration, the conditioned media were applied on their respective NT control cells to test cell proliferation induction. Figure 3, *A* and *B*, presents the results of these medium swap experiments using DU145 and LNCaP NT control cell lines. Concentrated RPMI growth medium was applied on cells as a methodology control. We observed that the conditioned media derived from PACE4 and PC7 knockdown cell lines led to significant growth reduction of both DU145 (39% and 35%, respectively) and LNCaP (35% and 30%, respectively). However, no significant difference was observed with the conditioned media obtained from the furin knockdown DU145 cell line. These data suggest that PACE4 and PC7 are more important in the activation of secreted growth factors than furin. To ascertain this hypothesis, we also tested the effect of conditioned media obtained from control DU145 cell lines (NT) and applied them to the PACE4- (Figure 3*C*) and PC7 (Figure 3*D*)–silenced DU145 cell lines. In both cases, this control conditioned medium rescued PACE4 and PC7 knockdown cell growth by 70% when compared to conditioned medium derived from the tested cell line (74% for PACE4 and 73% for PC7).

Only PACE4 Down-regulation Prevents Prostate Tumor Growth In Vivo *and Reduces Neovascularization*

We then tested the ability of furin-, PACE4-, and PC7-silenced DU145 and LNCaP cell lines to form tumor xenografts in immunodeficient mice after subcutaneous inoculations. Tumor growth was first monitored by periodically measuring their volume (Figure 4, *A* and *B*). As we previously reported, PACE4 silencing in DU145 cells led to a significant reduction in tumor growth where tumor volume was 60% smaller than controls (Figure 4*A*). However, no significant difference was observed for the furin and PC7 knockdown DU145 cell lines, even 33 days post-implantation (Figure 4*A*). These observations were identical for xenografts derived from LNCaP knockdown cell lines, where the phenotype was even more pronounced for the PACE4-silenced cells, as these cells were unable to form tumors bigger than 15% to 20% of the control tumor volumes (Figure 4*B*). Endpoint analyses were performed by excising and weighing tumors (Figure 4*C*). Tumors from LNCaP PACE4–silenced cells weighed 10 ± 2 mg, whereas tumors from control cells weighed 90 ± 20 mg (Figure 4*C*). No significant difference was observed for tumors derived from furin and PC7 knockdown LNCaP cells.

Because LNCaP cells secrete PSA, we verified whether tumor xenograft volumes correlated with plasmatic PSA concentrations [13]. Plasma samples from xenografted mice were collected on a weekly basis. As control, we first verified if the secretion of PSA from all knockdown lines was affected. As no significant variation in PSA

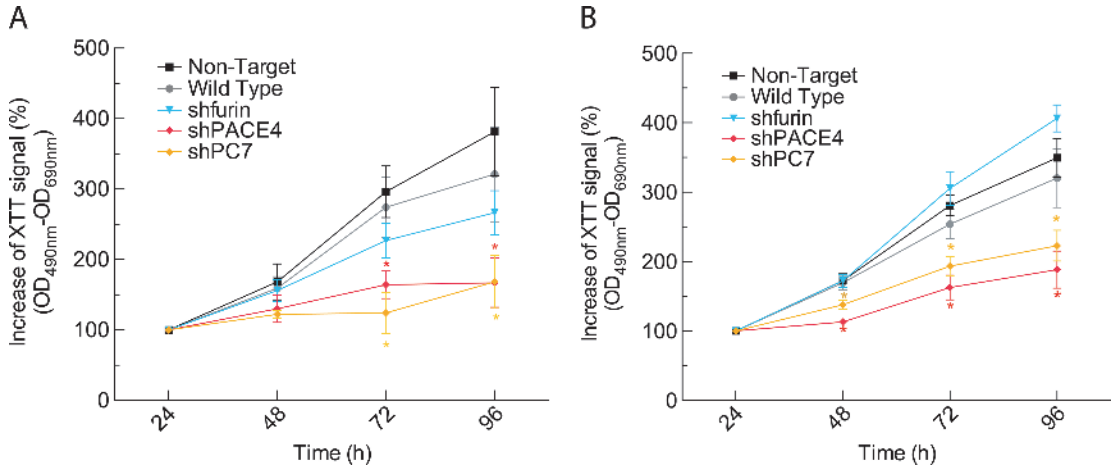

Figure 2. Cellular proliferation on PC knockdown. (A) DU145 cells (1×10^3 cells/well) or (B) LNCaP cells (3×10^3 cells/well) were plated in 96-well plates with, respectively, 5% and 10% FBS. Every 24 hours, XTT was added to each well and incubated 4 hours to monitor growth rates for each cell line. Values are means ± SEM ($n = 3$) of the increases of XTT signal ($OD_{490\ nm}$–$OD_{690\ nm}$) relative to the 24-hour reading for each cell line. *$P < .05$.

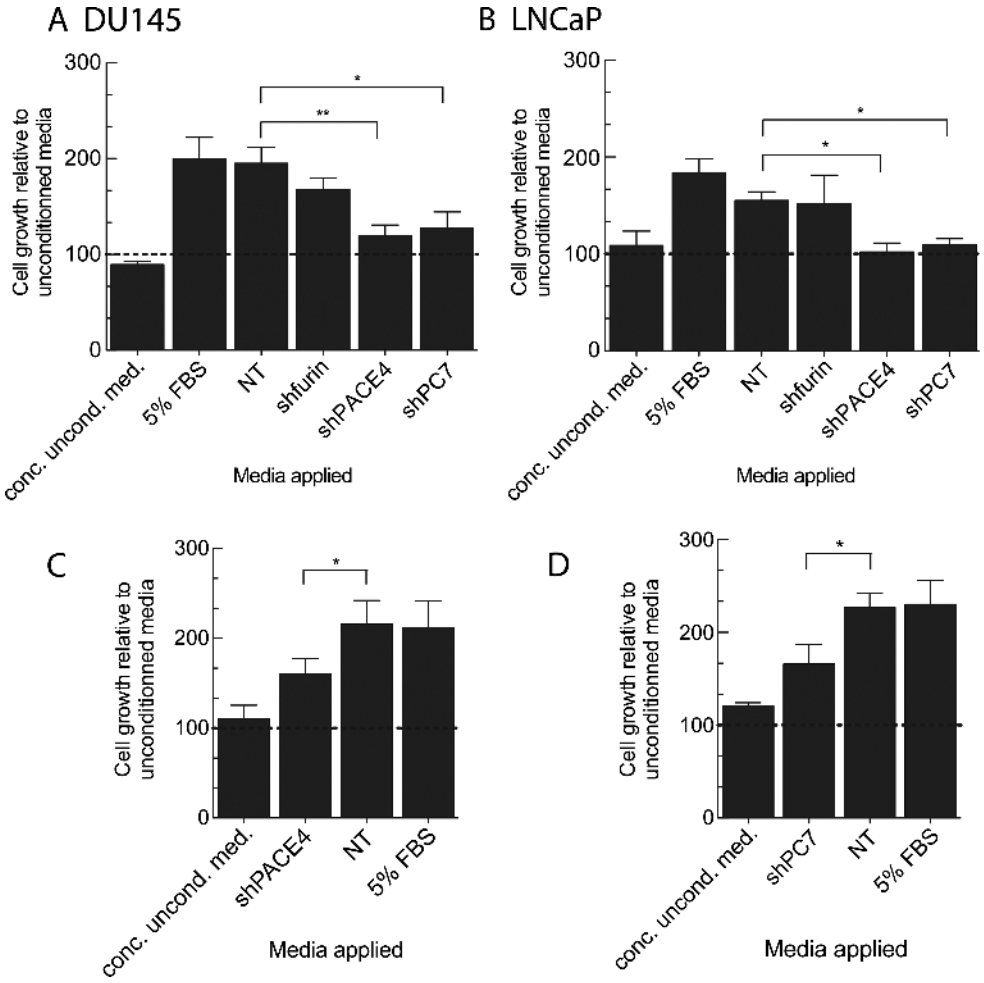

Figure 3. Mitogenic properties of secreted factors derived from PC knockdown cell lines. (A) DU145 and (B) LNCaP NT control cells (1.5×10^3 and 4.5×10^3 cells/well, respectively) were plated in 96-well plates with complete media. After 24 hours, media were replaced by either serum-free (uncond. med.), concentrated serum-free (conc. uncond. med.), or conditioned media derived from knockdown cell lines. *X*-axis labels correspond to the cell lines that produced the conditioned medium applied. After 48 hours, MTT reagent was added to each well, and following an incubation period of 4 hours, absorbance values ($OD_{550\ nm}$–$OD_{650\ nm}$) of cell lysates were read using a spectrophotometer. DU145 shPACE4 (C) and shPC7 (D) cell lines were plated and used to compare growth rates on conditioned medium application. Values are means ± SEM ($n = 3$) of the absorbance for each condition relative to serum-free medium-treated cells. *$P < .05$.

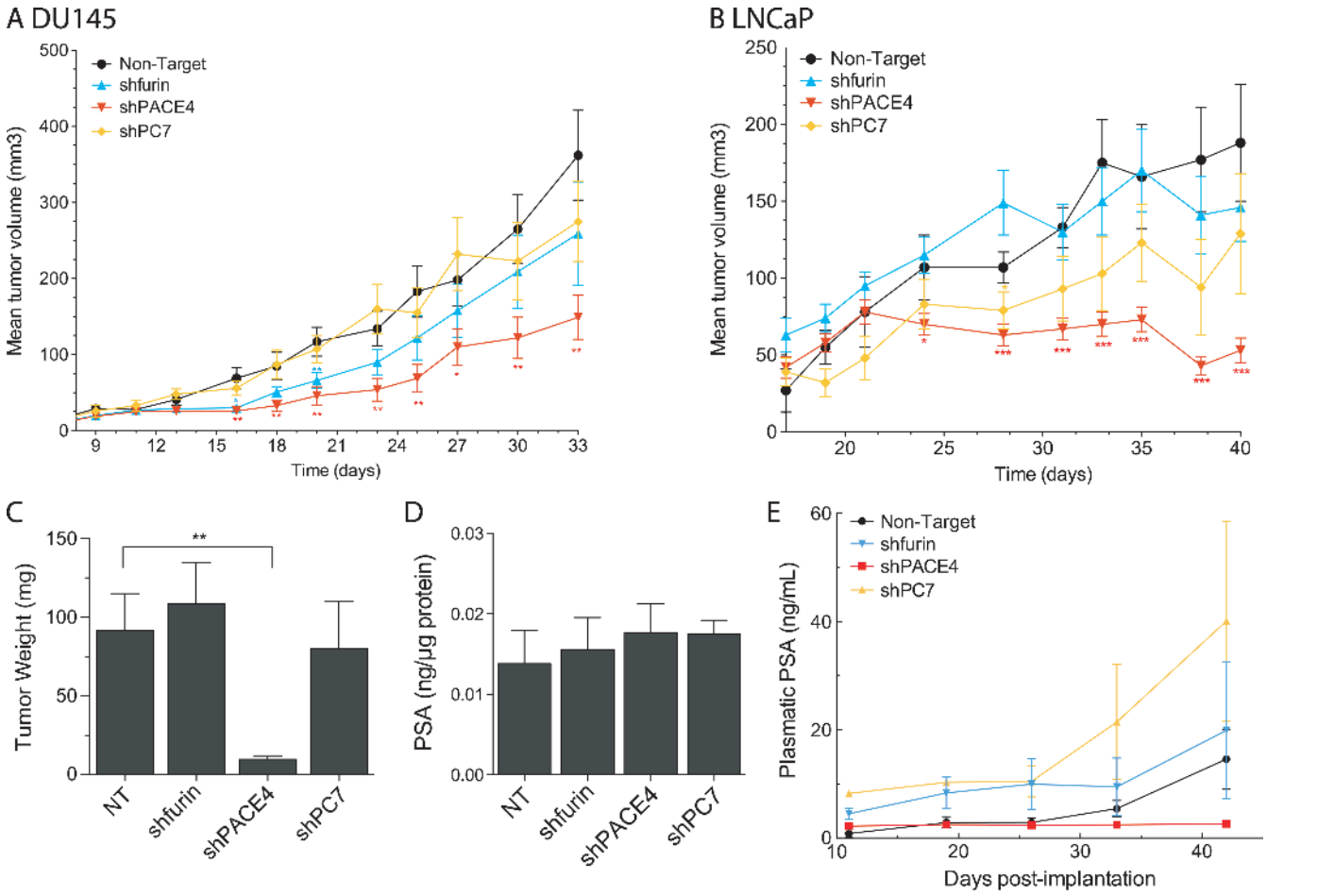

Figure 4. *In vivo* tumorigenicity assay of PC knockdown prostate cancer cell lines. (A) 3.0 × 10^6 DU145 cells and (B) 2.0 × 10^6 LNCaP cells were subcutaneously injected on both flanks and hips of four-week-old nu/nu male mice (four injections per mice; five mice per group). The length and the width of the tumors were measured periodically. Values shown are means ± SEM of tumor volumes for all tumors measured per mice group [volume = $(\text{width})^2 \times \text{length} \times \pi/6$]. (C) LNCaP tumor weight on excision from mice at the end of the experiment showing the remarkably smaller tumors generated by PACE4 knockdown cells. (D) Measurements of the PSA levels in the concentrated normalized conditioned medium from LNCaP cell lines (Figure 3) normalized on protein content determined by a BCA protein assay. (E) Plasmatic PSA concentrations from blood samples taken on a weekly basis during the xenograft experiment with LNCaP-derived cell lines. *$P < .05$, **$P < .01$, ***$P < .001$.

secretion was observed, we considered that PSA monitoring *in vivo* would correlate with tumor progression (Figure 4*D*). Figure 4*E* shows that PSA levels measured in the tumor-carrying mice ranged from 15 to 40 ng/ml for all mice except those with PACE4-silenced LNCaP xenografts, where background levels of 3 ng/ml were consistently measured. Our observations provide supporting data that these cells were unable to form tumors during the 40+-day experiments, as some tumors completely disappeared before the end of the experiment.

LNCaP cells normally form xenografts with a distinct dark red color, which is associated with extensive neovascularization [14,15]. However, PACE4-silenced LNCaP tumors lacked this characteristic darker color, as shown in Figure 5*A*. This reddish coloration is most probably due to erythrocytes within the tumor as visible on the H&E in Figure W2. The color of xenografts derived from furin and PC7 knockdowns were similar to the controls. MVDs shown in Figure 5*B* were calculated using CD34 immunostaining (Figure 5, *C* and *D*), a marker of endothelial cells in tumors [16]. The 80% reduction in MVD between NT and shPACE4 supported the notion that tumors derived from PACE4-silenced cells were less vascularized than the control tumors.

The Silencing of PACE4 in Prostate Cancer Cell Lines Enhances Quiescence in Tumor Xenografts

At the end of each xenograft formation assay, the tumors were excised and paraffin embedded for further IHC analyses using cell proliferation markers. As shown in Figure 6, *A* and *B*, Ki67 immunostaining, a strict marker of cellular proliferation, revealed a statistically reduced number of cells undergoing cell cycle progression in the tumors issued from PACE4-silenced cells (50% and 90% reduction in Ki67 proliferation index compared to controls, for DU145 and LNCaP cell lines, respectively). The DU145 tumors silenced for furin and PC7 had a very slight, but significant, reduction of their proliferation index (around 15%). No significant difference was observed for the furin and PC7 knockdown LNCaP xenografts.

We also tested $p27^{KIP}$ immunostaining, a cyclin-dependent kinase (CDK) inhibitory protein implicated in the blocking of the cell cycle transition from the G_0/G_1 to S phase transition during cell quiescence and subsequently degraded on mitogenic signaling [17]. Higher immunolabeling of $p27^{KIP}$ was observed only in xenografts resulting from PACE4-silenced cells. Tumors derived from PACE4-silenced

DU145 cells had more than two-fold increase in $p27^{KIP}$ whereas the PACE4-silenced LNCaP cells showed a four-fold increase (Figure 6, *C* and *D*), while no significant changes were observed in other PC-silenced cell lines.

We also tested the EGF signaling pathway, as a previous report showed a link between this signaling pathway and PC7 [18] and also because EGFR has been reported to enhance prostate cancer cell growth and invasiveness [19,20]. EGFR immunostaining remained relatively unchanged in xenografts derived from PACE4 or furin knockdown DU145 or LNCaP cells. However, EGFR levels were much higher in xenografts issued from PC7-silenced DU145 and LNCaP cells, with respective increases of 75% and 150% in comparison to control tumors (Figure 6, *E* and *F*). To determine whether these higher levels of EGFR were contributing to the restored proliferative capabilities of PC7 knockdown xenografts, we immunoblotted both EGFR and phosphorylated EGFR on DU145 xenograft protein extracts. Figure 7*A* confirms that not only EGFR but also phosphorylated EGFR (PS1070-EGFR; phosphorylation on Ser^{1070}) protein levels were truly increased in PC7 knockdown tumors, whereas in PACE4 and furin knockdown xenografts, levels remained statistically unchanged for both proteins. These results are in agreement with immunostaining results (Figure 6*E*). We also tested furin, PACE4, and PC7 mRNA levels in the tumor xenografts (Figure 7*B*) and the changes observed correlated with the Western blot (Figure 7*A*) and immunostaining analyses even if statistical significance was not reached (Figure 6*E*). Thus, EGFR protein and activation levels increase only in xenografts derived from PC7 knockdown cell lines. However, when we went back to verify EGFR and phosphorylated EGFR proteins in the original cell lines, no changes were observed for both EGFR and phosphorylated EGFR levels in the PC7 knockdown cell lines or in any other PC knockdown cell lines (Figure 7*C*). These results support the observed disparity between *in vitro* and *in vivo* growth conditions having an impact on cell behavior.

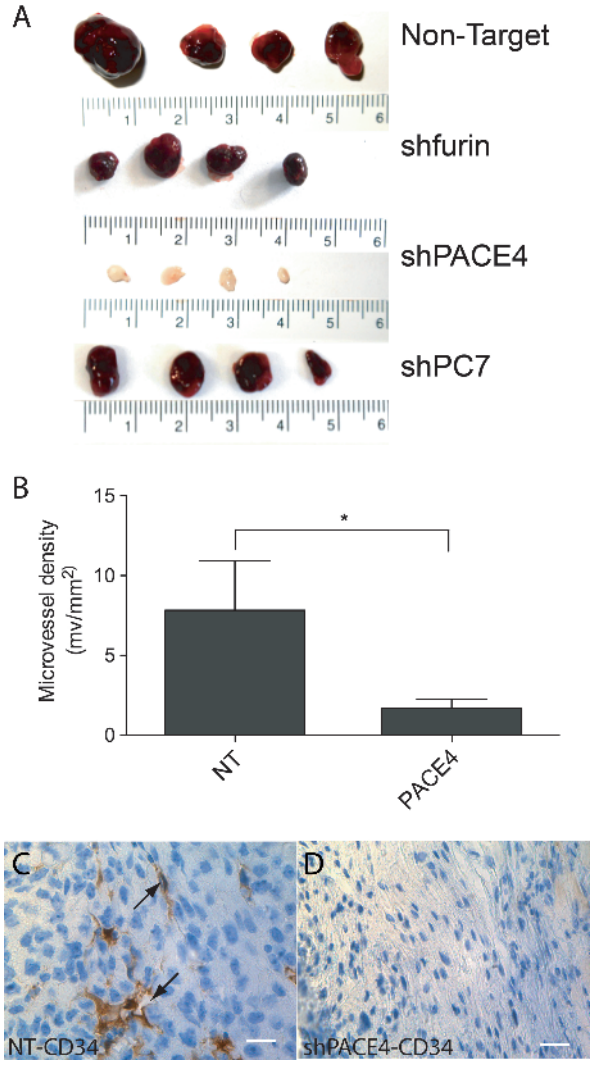

Figure 5. Xenograft MVD of tumors derived from LNCaP cell lines. (A) Representative LNCaP tumors showing the distinctive white color of tumors derived from PACE4 knockdown cells. (B) MVD calculated for the NT and shPACE4 tumors using CD34 immunostaining. CD34 staining of NT (C) and (D) shPACE4 LNCaP tumors. Arrows point to microvessel lumens. Scale represents 25 μm. *$P < .05$.

Discussion

The PCs are thought to play important roles in cancer development and progression. While they are essential for normal cells, cancer cells also appear to heavily depend on their processing activities for maintained survival and progression. However, it is unclear if PCs are constitutive players or have distinct functions in specific steps of cancer progression. Distinct and redundant PC functions remain an important issue, not only at the individual substrate processing level but also in more global cellular processes. Therefore, in the context of providing evidence for PCs as druggable targets in cancer, answers to these questions are essential. Our previous work suggested that PACE4 plays a major role in prostate cancer, but, until now, we were unable to compare functional aspects with other expressed PCs. We now provide evidence that PACE4 has a distinct role on prostate cancer cell proliferation that is not sustained by furin or PC7 redundant functions.

Attempts to define prostate cancer regulatory networks have been made and lead to complex signaling networks interconnected at various points of convergence [21]. The data highlight the critical roles of autocrine and paracrine growth factors in tumor progression. Such cellular modulators are part of the epithelial and stromal interactions, which are crucial in the complex mechanisms leading to tumor progression and metastasis [22–24]. Growth factors are especially important actors in prostate carcinoma, as they are known to substitute androgens by multiple alternative mechanisms leading to preserved proliferative response [25–27]. As with the tumor microenvironment, the extracellular matrix is also extensively remodeled in terms of integrin and matrix metalloproteinase composition during prostate carcinogenesis and is associated with tumor invasiveness and metastatic dissemination of cancer cells, which is the major cause of cancer-associated mortality [28,29]. Many of these tumor progression–related proteins are known to be concurrently overexpressed in prostatic neoplasms [30–32]. However, the multiple efforts made to develop targeted therapeutic agents were mostly unsuccessful [33]. As we now understand more about cancer progression from the point of view of a system's biology approach, we have come to realize that many of these tumor microenvironment actors share common mechanisms of biologic activation, being synthesized as inactive proproteins. Indeed, most growth factors [e.g., EGF, transforming growth factor β, insulin-like growth factor I/II (IGF-I/II)], growth factor receptors (e.g., IGF1R and Notch1), some integrins, and matrix metalloproteinases require at least one activating proteolytic cleavage achieved by the PCs [34].

In spite of this understanding, PCs have not been widely appreciated as drug targets in cancer because of several factors. First, PC enzymes

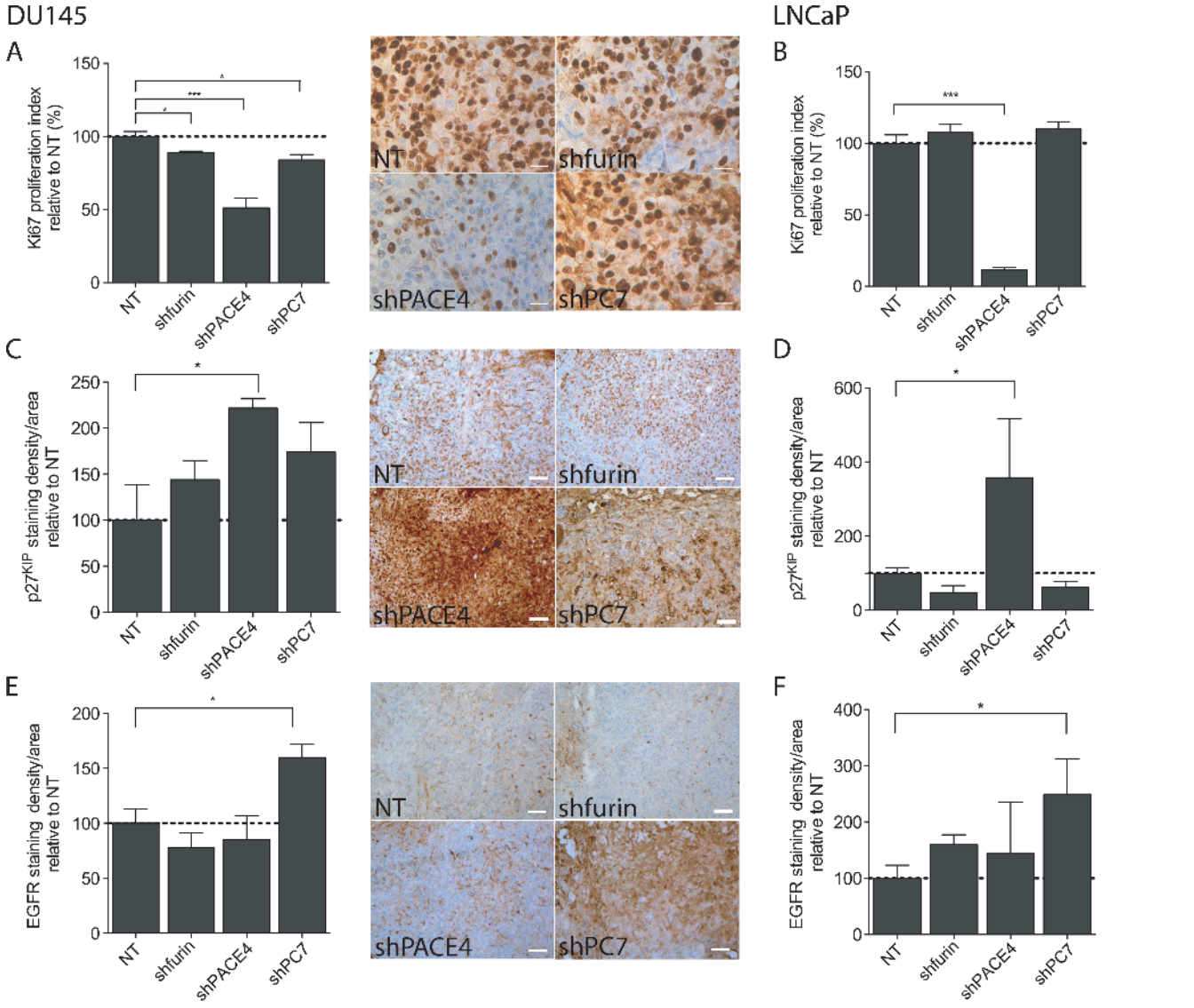

Figure 6. IHC against cell cycle markers and EGFR protein for DU145 and LNCaP tumor xenografts. (A and B) Ki67, (C and D) $p27^{KIP}$, and (E and F) EGFR IHC quantifications relative to respective NT control in both DU145- and LNCaP-derived tumors. Ki67 proliferation index was determined by counting cells with positive nuclear staining in the representative field. $p27^{KIP}$ and EGFR immunostaining densities relative to tumor areas, which were confirmed by counterstaining (H&E and positive marker; p53 for DU145 and PSA for LNCaP, respectively), were quantified using CMYK quantification. Pictures are representative fields of DU145 staining for each tumor type [original magnification, ×400 (Ki67) and ×100 (others)]. Scale bar represents 25 μm (Ki67) and 100 μm (others). *$P < .05$, ***$P < .001$.

are widely expressed in tissues and it has been speculated that their systemic inhibition would be a drawback, causing important secondary effects. Second, it has been anticipated that beneficial effects might be limited because of known redundant functions among the PCs. As a counterpoint to both arguments, PCs can be considered as useful pharmacological targets if redundancy serves to preserve the overall functions of normal cells, whereas target cells, such as cancer cells, may be more dependent on a single PC for survival and may thus be vulnerable to the inhibition of that PC [2]. This idea is compatible if that PC sits at a strategic hub that regulates the activities of multiple cancer-promoting proteins. It is therefore possible to imagine that a single compound targeting a single PC for inhibition, for example, PACE4, could have a major impact on cancer progression. This could occur through the simultaneous inhibition of a large number of growth factors, by blockade of the processing activation step, as a general way of reducing many associated downstream signaling pathways. Indeed, growth factor signaling pathways have been proposed as key therapeutic targets in prostate cancer [26,35,36], but their simultaneous inhibition has been problematic considering their high number.

In this study, we tested whether PACE4 is a unique target in prostate cancer progression and whether future anticancer compounds should be designed to also target other PCs. Molecular silencing techniques are the most effective way to obtain such proofs of concept. We used a lentivirus shRNA delivery approach that most appropriately permitted us to rapidly produce cell lines with significantly silenced PC mRNA expression levels (typically 80–90% reductions). PACE4-silenced DU145 cells using this lentivirus approach behaved just like the switch on/off adapter (SOFA)-hepatitis delta virus ribozyme (HDVRz)-mediated PACE4-silenced DU145 cells in our previous report [10], solidifying our contention of the vital role of PACE4 in

prostate cancer cell survival. The use of two completely different methodologies resulting in identical data nullifies potential arguments that observed antiproliferative effects are due to major cell aberrations or toxicity due to technical manipulations. Additionally, similar antiproliferation effects were observed when PACE4 was silenced in LNCaP cells.

In an attempt to determine how PACE4 silencing works in prostate cancer cells, we carried out medium swap experiments, providing proof of the attenuated secretion of active mitogenic growth factors (Figure 3). The lack of mitogenic activity was associated with higher cell quiescence states characterized by the increase of $p27^{KIP}$, as observed in the resulting tumor xenografts (Figure 6). $p27^{KIP}$ is a CDK inhibitor protein that binds and prevents the activation of cyclin E–CDK2 or cyclin D–CDK4 complexes and thus controls the cell cycle progression at the G_1 phase. PACE4 silencing in DU145 and LNCaP cells was also associated with a considerable decrease in Ki67-positive cells in tumor xenografts. Ki67 is a nuclear protein associated with ribosomal RNA transcription and is a cellular marker that is strictly associated with cell proliferation. Though the sum of these data leads us to conclude that PACE4 has a critical role in prostate cancer cell proliferation. Additionally, we propose that PACE4 is a hub protein for the proliferative response in prostate neoplasia [37]. The concept of hub proteins has been put forth for protein interactors and deletion of such protein has direct consequences often resulting in lethality. In some systems, these hub proteins are considered as "master switches" controlling the regulation of entire pathways. It should be noted that we propose PACE4 as a hub protein only in the pathophysiological processes of prostate cancer cells and not in normal cells. The principal reason we do not include normal cells is related to the results obtained with PACE4 knockout mice. PACE4 knockout mice are viable, although it was initially reported that lethality occurred in 25% of mutant homozygous offspring, while others exhibit craniofacial abnormalities [38]. However, the penetrance of this phenotype appears to be rather low, as the deletion of PACE4 results in normal mice without any lethality when performed in the C57BL/6 instead of the SV129 background [39]. As prostate cancer cells are known for their extreme genetic heterogeneity [40,41], it remains a challenge to define hub proteins in tumor maintenance processes that could serve as effective targets. Downstream pathways that are insured by hubs that are involved in proteolytic activation could be suitable for targeted therapies, with the aim to treat primarily cancer cells without affecting normal tissues [42].

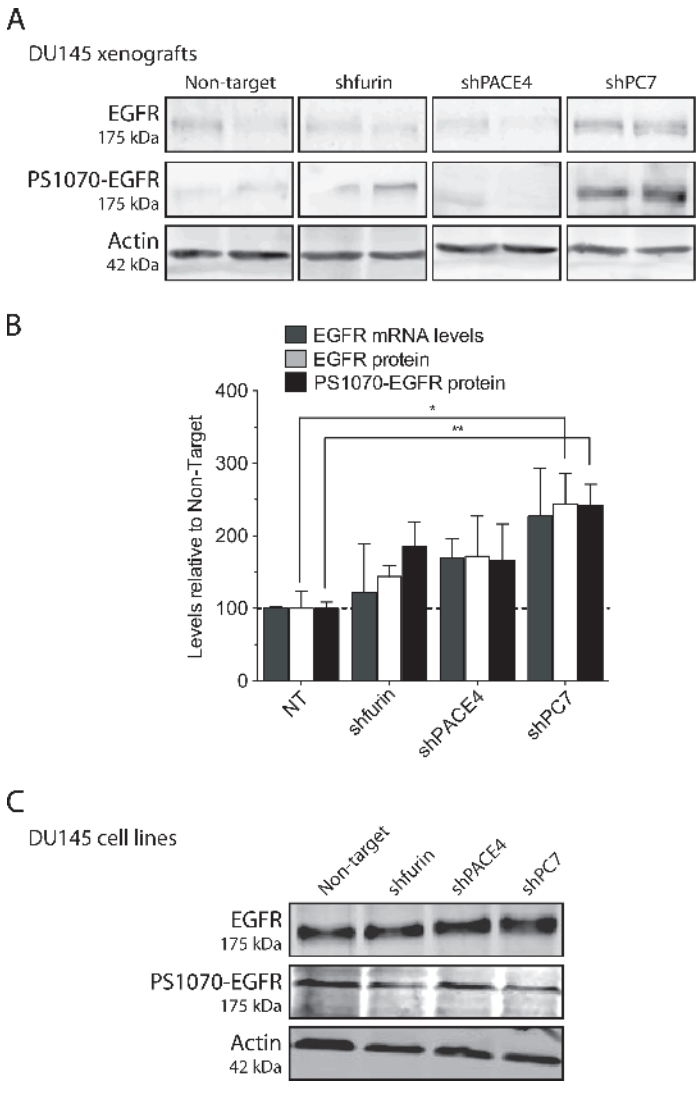

Figure 7. EGFR Western blots on DU145-derived tumors. (A and B) Tumor lysates were analyzed for their EGFR and phospho-Ser^{1070}-EGFR contents by Western blots and for their EGFR mRNA expression levels by real-time qPCR. Two tumors per knockdown/control were assayed using β-actin as a loading control for Western blots and as the reference gene for qPCR. (C) Cell lysates were also assessed for their protein levels by Western blots. $^*P < .05$, $^{**}P < .01$.

In regard to the other two PCs highly expressed in prostate cancer cells, namely, furin and PC7, it was important to verify if they also had important roles to play in tumor progression. In previous studies, furin was described as having an important association with cancer/tumorigenesis processes as it cleaves many cancer-associated protein precursors [34]. Surprisingly, in prostate cancer cells, we did not observe any effects following furin silencing, as the cells were entirely viable and formed xenografts with identical characteristics to control cells. Previous studies have reported that a full furin knockout is lethal to mice [43], which has led to the still accepted suggestion that inhibition of furin in any cell would lead to cell death. However, other studies have shown that the lethality of furin inhibition during early phases of embryonic development can be overcome under physiological conditions, as demonstrated by conditional furin knockouts [44,45]. This suggests that cells can survive without furin, most likely as other PCs are providing sufficient compensatory functions. In regard to cancer cells, the situation remains confused, as, for example, it has been recently reported that furin overexpression in hepatocellular carcinoma cells was associated with growth reduction [46,47]. Moreover, high furin levels in clinical hepatocellular carcinoma specimens were correlated with a better postoperative disease–free survival. The apparent paradoxical results lead us to state that general conclusions about a single PC are not applicable to all cancer types. A PC may fulfill a specific role in one cancer cell type but not in another. Additionally, predictions solely based on genetic models or cultured cells may also not be realistic.

In regard to PC7, we observed paradoxical effects between the *in vitro* and *in vivo* phenotypes of the PC7-silenced DU145 and LNCaP cells. For both cell lines, *in vitro* proliferation rates were reduced, whereas *in vivo* xenograft growth was unaffected and comparable to control cells (Figures 2 and 4). In an attempt to understand these observations, we tested various cellular markers using IHC and molecular analysis of both cell lines and derived tumors (Figures 6 and 7). Xenografts from PC7-silenced LNCaP and DU145 cells displayed highly increased

levels of EGFR, as well as EGFR phosphorylated on Ser^{1070} (i.e., its activated form). This was not observed when these same cell lines were under cell culture conditions. Combined with the restoration of their Ki67 proliferation index in these xenografts, we conclude that PC7 inhibition improves pro-proliferative cell capabilities *in vivo*. Indeed, EGFR has been described as an important driver of DU145 cell proliferation and invasiveness both *in vitro* and *in vivo* [19,20,48]. In LNCaP cells, it is well known that mitogenic steroid concentrations induce cell proliferation by mediating an increase in EGFR protein, making them more sensitive to surrounding ligands [49,50]. Thus, PC7 may be implicated in growth inhibitory mechanisms, which are only discernible *in vivo*.

From the present study, we conclude that PACE4 carries out a distinct function in prostate cancer cells, critical for cell proliferation, tumor progression, and vascularization, as these functions were not duplicated by furin or PC7. It was conceivable, and even likely, that cleavage sites in cancer-associated proteins processed by PACE4 could be redundantly processed by furin and PC7. However, blockade of furin and PC7 did not translate into the blockade of a global function such as *in vivo* tumor progression, whereas that of PACE4 does. From a therapeutic point of view, we conclude that drugs targeting PACE4 should be highly effective in prostate cancer and do not need to encompass the additional inhibition of other PCs. PACE4 is a critical driver in the prostatic neoplastic process and strengthens its position as a novel pharmacological target in prostate cancer.

Acknowledgments

The authors thank Leonid Volkov and Vanessa Couture for helpful discussions and technical assistance.

References

[1] Seidah NG and Prat A (2012). The biology and therapeutic targeting of the proprotein convertases. *Nat Rev Drug Discov* **11**, 367–383.

[2] Couture F, D'Anjou F, and Day R (2011). On the cutting edge of proprotein convertase pharmacology: from molecular concepts to clinical applications. *Biomol Concepts* **2**, 421–438.

[3] Hanahan D and Weinberg RA (2011). Hallmarks of cancer: the next generation. *Cell* **144**, 646–674.

[4] Fu J, Bassi DE, Zhang J, Li T, Nicolas E, and Klein-Szanto AJ (2012). Transgenic overexpression of the proprotein convertase furin enhances skin tumor growth. *Neoplasia* **14**, 271–282.

[5] Dogar AM, Towbin H, and Hall J (2011). Suppression of latent transforming growth factor (TGF)-β1 restores growth inhibitory TGF-β signaling through microRNAs. *J Biol Chem* **286**, 16447–16458.

[6] Mahloogi H, Bassi DE, and Klein-Szanto AJ (2002). Malignant conversion of non-tumorigenic murine skin keratinocytes overexpressing PACE4. *Carcinogenesis* **23**, 565–572.

[7] McColl BK, Paavonen K, Karnezis T, Harris NC, Davydova N, Rothacker J, Nice EC, Harder KW, Roufail S, Hibbs ML, et al. (2007). Proprotein convertases promote processing of VEGF-D, a critical step for binding the angiogenic receptor VEGFR-2. *FASEB J* **21**, 1088–1098.

[8] Bassi DE, Lopez De Cicco R, Cenna J, Litwin S, Cukierman E, and Klein-Szanto AJ (2005). PACE4 expression in mouse basal keratinocytes results in basement membrane disruption and acceleration of tumor progression. *Cancer Res* **65**, 7310–7319.

[9] American cancer statistics (2012). *American Cancer Society*. Available at: http://www.cancer.org.

[10] D'Anjou F, Routhier S, Perreault JP, Latil A, Bonnel D, Fournier I, Salzet M, and Day R (2011). Molecular validation of PACE4 as a target in prostate cancer. *Transl Oncol* **4**, 157–172.

[11] Yuasa K, Masuda T, Yoshikawa C, Nagahama M, Matsuda Y, and Tsuji A (2009). Subtilisin-like proprotein convertase PACE4 is required for skeletal muscle differentiation. *J Biochem* **146**, 407–415.

[12] Pham NA, Morrison A, Schwock J, Aviel-Ronen S, Iakovlev V, Tsao MS, Ho J, and Hedley DW (2007). Quantitative image analysis of immunohistochemical stains using a CMYK color model. *Diagn Pathol* **2**, 8.

[13] Gleave ME, Hsieh JT, Wu HC, von Eschenbach AC, and Chung LW (1992). Serum prostate specific antigen levels in mice bearing human prostate LNCaP tumors are determined by tumor volume and endocrine and growth factors. *Cancer Res* **52**, 1598–1605.

[14] Igawa T, Lin FF, Rao P, and Lin MF (2003). Suppression of LNCaP prostate cancer xenograft tumors by a prostate-specific protein tyrosine phosphatase, prostatic acid phosphatase. *Prostate* **55**, 247–258.

[15] Okamoto R, Delansorne R, Wakimoto N, Doan NB, Akagi T, Shen M, Ho QH, Said JW, and Koeffler HP (2012). Inecalcitol, an analog of 1α,25(OH)(2) D(3), induces growth arrest of androgen-dependent prostate cancer cells. *Int J Cancer* **130**, 2464–2473.

[16] Bettencourt MC, Bauer JJ, Sesterhenn IA, Connelly RR, and Moul JW (1998). CD34 immunohistochemical assessment of angiogenesis as a prognostic marker for prostate cancer recurrence after radical prostatectomy. *J Urol* **160**, 459–465.

[17] Chu IM, Hengst L, and Slingerland JM (2008). The Cdk inhibitor p27 in human cancer: prognostic potential and relevance to anticancer therapy. *Nat Rev Cancer* **8**, 253–267.

[18] Rousselet E, Benjannet S, Marcinkiewicz E, Asselin MC, Lazure C, and Seidah NG (2011). Proprotein convertase PC7 enhances the activation of the EGF receptor pathway through processing of the EGF precursor. *J Biol Chem* **286**, 9185–9195.

[19] Turner T, Chen P, Goodly LJ, and Wells A (1996). EGF receptor signaling enhances *in vivo* invasiveness of DU-145 human prostate carcinoma cells. *Clin Exp Metastasis* **14**, 409–418.

[20] Xie H, Turner T, Wang MH, Singh RK, Siegal GP, and Wells A (1995). *In vitro* invasiveness of DU-145 human prostate carcinoma cells is modulated by EGF receptor-mediated signals. *Clin Exp Metastasis* **13**, 407–419.

[21] Altieri DC, Languino LR, Lian JB, Stein JL, Leav I, van Wijnen AJ, Jiang Z, and Stein GS (2009). Prostate cancer regulatory networks. *J Cell Biochem* **107**, 845–852.

[22] Ware JL (1993). Growth factors and their receptors as determinants in the proliferation and metastasis of human prostate cancer. *Cancer Metastasis Rev* **12**, 287–301.

[23] Barton J, Blackledge G, and Wakeling A (2001). Growth factors and their receptors: new targets for prostate cancer therapy. *Urology* **58**, 114–122.

[24] Dayyani F, Gallick GE, Logothetis CJ, and Corn PG (2011). Novel therapies for metastatic castrate-resistant prostate cancer. *J Natl Cancer Inst* **103**, 1665–1675.

[25] Ishii K, Imamura T, Iguchi K, Arase S, Yoshio Y, Arima K, Hirano K, and Sugimura Y (2009). Evidence that androgen-independent stromal growth factor signals promote androgen-insensitive prostate cancer cell growth *in vivo*. *Endocr Relat Cancer* **16**, 415–428.

[26] Lamont KR and Tindall DJ (2011). Minireview: alternative activation pathways for the androgen receptor in prostate cancer. *Mol Endocrinol* **25**, 897–907.

[27] Zhu ML and Kyprianou N (2008). Androgen receptor and growth factor signaling cross-talk in prostate cancer cells. *Endocr Relat Cancer* **15**, 841–849.

[28] Lokeshwar BL (1999). MMP inhibition in prostate cancer. *Ann N Y Acad Sci* **878**, 271–289.

[29] Fornaro M, Manes T, and Languino LR (2001). Integrins and prostate cancer metastases. *Cancer Metastasis Rev* **20**, 321–331.

[30] Mueller MM and Fusenig NE (2004). Friends or foes—bipolar effects of the tumour stroma in cancer. *Nat Rev Cancer* **4**, 839–849.

[31] De Wever O, Demetter P, Mareel M, and Bracke M (2008). Stromal myofibroblasts are drivers of invasive cancer growth. *Int J Cancer* **123**, 2229–2238.

[32] Desmouliere A, Guyot C, and Gabbiani G (2004). The stroma reaction myofibroblast: a key player in the control of tumor cell behavior. *Int J Dev Biol* **48**, 509–517.

[33] Karlou M, Tzelepi V, and Efstathiou E (2010). Therapeutic targeting of the prostate cancer microenvironment. *Nat Rev Urol* **7**, 494–509.

[34] Khatib A-M, Siegfried G, Chrétien M, Metrakos P, and Seidah NG (2002). Proprotein convertases in tumor progression and malignancy: novel targets in cancer therapy. *Am J Pathol* **160**, 1921–1935.

[35] Culig Z, Hobisch A, Cronauer MV, Radmayr C, Hittmair A, Zhang J, Thurnher M, Bartsch G, and Klocker H (1996). Regulation of prostatic growth and function by peptide growth factors. *Prostate* **28**, 392–405.

[36] Russell PJ, Bennett S, and Stricker P (1998). Growth factor involvement in progression of prostate cancer. *Clin Chem* **44**, 705–723.

[37] He X and Zhang J (2006). Why do hubs tend to be essential in protein networks? *PLoS Genet* **2**, e88.
[38] Constam DB and Robertson EJ (2000). SPC4/PACE4 regulates a TGFβ signaling network during axis formation. *Genes Dev* **14**, 1146–1155.
[39] Malfait AM, Seymour AB, Gao F, Tortorella MD, Le Graverand-Gastineau MP, Wood LS, Doherty M, Doherty S, Zhang W, Arden NK, et al. (2012). A role for PACE4 in osteoarthritis pain: evidence from human genetic association and null mutant phenotype. *Ann Rheum Dis* **71**, 1042–1048.
[40] Andreoiu M and Cheng L (2010). Multifocal prostate cancer: biologic, prognostic, and therapeutic implications. *Hum Pathol* **41**, 781–793.
[41] Vogelstein B and Kinzler KW (2004). Cancer genes and the pathways they control. *Nat Med* **10**, 789–799.
[42] Sawyers C (2004). Targeted cancer therapy. *Nature* **432**, 294–297.
[43] Roebroek AJ, Umans L, Pauli IG, Robertson EJ, van Leuven F, Van de Ven WJ, and Constam DB (1998). Failure of ventral closure and axial rotation in embryos lacking the proprotein convertase furin. *Development* **125**, 4863–4876.
[44] Roebroek AJ, Taylor NA, Louagie E, Pauli I, Smeijers L, Snellinx A, Lauwers A, Van de Ven WJ, Hartmann D, and Creemers JW (2004). Limited redundancy of the proprotein convertase furin in mouse liver. *J Biol Chem* **279**, 53442–53450.
[45] De Vos L, Declercq J, Rosas GG, Van Damme B, Roebroek A, Vermorken F, Ceuppens J, van de Ven W, and Creemers J (2008). MMTV-cre-mediated fur inactivation concomitant with PLAG1 proto-oncogene activation delays salivary gland tumorigenesis in mice. *Int J Oncol* **32**, 1073–1083.
[46] Huang YH, Lin KH, Liao CH, Lai MW, Tseng YH, and Yeh CT (2012). Furin overexpression suppresses tumor growth and predicts a better postoperative disease-free survival in hepatocellular carcinoma. *PLoS One* **7**, e40738.
[47] Lapierre M, Siegfried G, Scamuffa N, Bontemps Y, Calvo F, Seidah NG, and Khatib AM (2007). Opposing function of the proprotein convertases furin and PACE4 on breast cancer cells' malignant phenotypes: role of tissue inhibitors of metalloproteinase-1. *Cancer Res* **67**, 9030–9034.
[48] Sherwood ER, Van Dongen JL, Wood CG, Liao S, Kozlowski JM, and Lee C (1998). Epidermal growth factor receptor activation in androgen-independent but not androgen-stimulated growth of human prostatic carcinoma cells. *Br J Cancer* **77**, 855–861.
[49] Schuurmans AL, Bolt J, Voorhorst MM, Blankenstein RA, and Mulder E (1988). Regulation of growth and epidermal growth factor receptor levels of LNCaP prostate tumor cells by different steroids. *Int J Cancer* **42**, 917–922.
[50] Schuurmans AL, Bolt J, and Mulder E (1989). Androgen receptor-mediated growth and epidermal growth factor receptor induction in the human prostate cell line LNCaP. *Urol Int* **44**, 71–76.

Table W1. Specific shRNA Silencing Sequences.

Number*	Target Gene	Sequence	TRC Number†
I	PACE4	CGGGTCATAAAGTTAGCCATT	TRCN0000075248
II		GCGTGGATGAACCTGAGAAAT	TRCN0000075249
III		CCTGGAAGATTACTACCATTT	TRCN0000075250
IV		CCACGATATGATGCCAGCAAT	TRCN0000075251
V		GAGTGCATTCACTGTGCGAAA	TRCN0000075252
VI	Furin	CCTGTCCCTCTAAAGCAATAA	TRCN0000075238
VII		CCGCCTTTATCAAAGACCAGA	TRCN0000075239
VIII		CAGTATCTACACGCTGTCCAT	TRCN0000075240
IX		GAGTGGGTCCTAGAGATTGAA	TRCN0000075241
X		CCACATGACTACTCCGCAGAT	TRCN0000075242
XI	PC7	GCCTCCATTATCCATTCCCAA	TRCN0000072393
XII		GCACTATCAGATCAATGACAT	TRCN0000072394
XIII		CGCATGCCTTTCTATGCAGAA	TRCN0000072395
XIV		CTGGACATCTGTCCCTTACTT	TRCN0000072396
XV		CCAGGACATTGCACCCAACTA	TRCN0000072397

shRNAs in **bold** are the ones selected for this study because of their higher efficiency.
*shRNA numbers used for Figure W1.
†TRC number from Sigma–Aldrich for human genes.

Table W2. qPCR Primer Sequences.

Gene	Protein	Primer Sequences	Product Size (bp)
ACTB	β-Actin	Forward: 5′-CAGAGCCTCGCCTTTGCCGATC-3′ Reverse: 5′-CGATGCCGTGCTCGATGGGG-3′	280
PCSK3	Furin	Forward: 5′-GTGGCGACCTGGCCATCCAC-3′ Reverse: 5′-AGGTACGGGCAGCCCCTCAG-3′	251
PCSK6	PACE4	Forward: 5′-CACCTGCTAGTGAAGACATCC-3′ Reverse: 5′-AACGAGAGCTTCTGCGTCCAC-3′	122
PCSK7	PC7	Forward: 5′-GGGTCACCAACGAGGCAGGC-3′ Reverse: 5′-CCCCCAGCATCGCACAGTGG-3′	391
EGFR	EGFR	Forward: 5′-CCTGGTCTGGAAGTACGCAG-3′ Reverse: 5′-GCGATGGACGGGATCTTAGG-3′	126

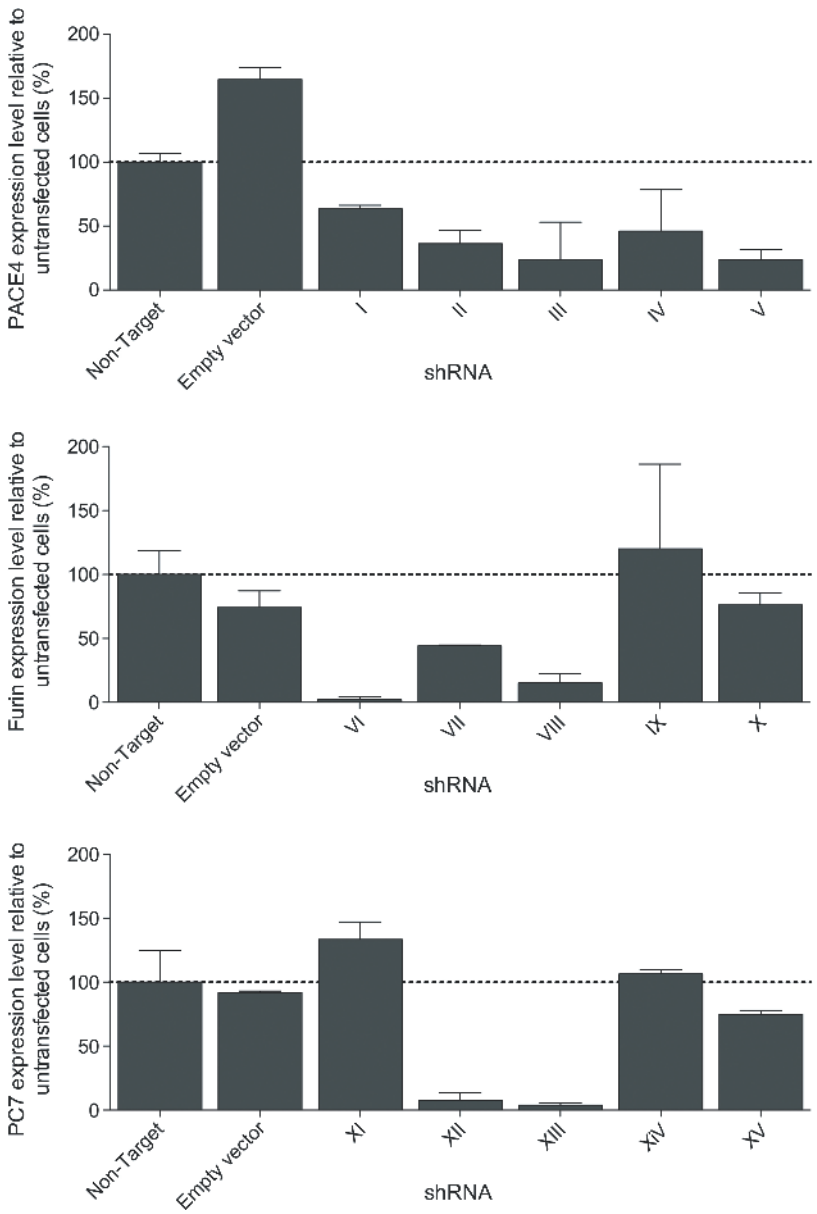

Figure W1. shRNA efficiency screening on DU145 cells. Northern blot hybridization densitometry of furin, PACE4, and PC7 mRNA relative to 18S RNA on total mRNA extracted from DU145 transfectants for the five shRNAs targeting furin (top), PACE4 (middle), and PC7 (bottom). Radioactive probes used are the same as in [10] (for shRNA numbers, refer to Table W1).

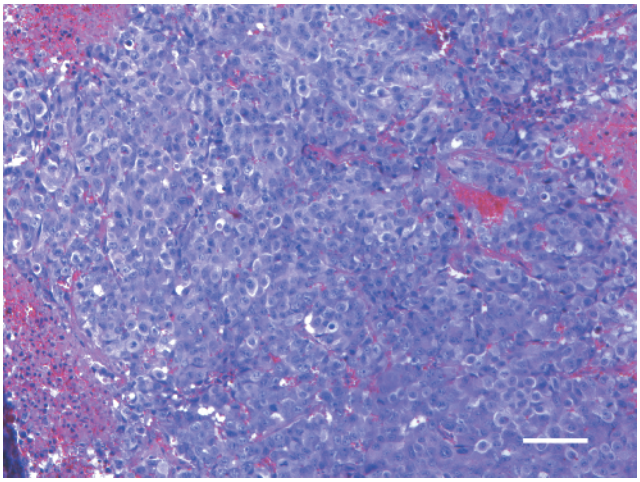

Figure W2. H&E staining on LNCaP tumors. H&E staining confirms the high vascularization of LNCaP tumor (NT on this picture), as multiple erythrocytes can be observed (red cells lacking purple nucleus) among the tumor cells within the tumors. Scale bar represents 100 μm.